

**Special Issue: Manufacturing of Advanced
Biodegradable Polymeric Components**

Guest Editors: Prof. Roberto Pantani (University of Salerno) and
Prof. Lih-Sheng Turng (University of Wisconsin-Madison)

EDITORIAL

Manufacturing of advanced biodegradable polymeric components

R. Pantani and L.-S. Turng, *J. Appl. Polym. Sci.* 2015, DOI: [10.1002/app.42889](https://doi.org/10.1002/app.42889)

REVIEWS

Heat resistance of new biobased polymeric materials, focusing on starch, cellulose, PLA, and PHA

N. Peelman, P. Ragaert, K. Ragaert, B. De Meulenaer, F. Devlieghere and Ludwig Cardon, *J. Appl. Polym. Sci.* 2015, DOI: [10.1002/app.42305](https://doi.org/10.1002/app.42305)

Recent advances and migration issues in biodegradable polymers from renewable sources for food packaging

P. Scarfato, L. Di Maio and L. Incarnato, *J. Appl. Polym. Sci.* 2015, DOI: [10.1002/app.42597](https://doi.org/10.1002/app.42597)

3D bioprinting of photocrosslinkable hydrogel constructs

R. F. Pereira and P. J. Bartolo, *J. Appl. Polym. Sci.* 2015, DOI: [10.1002/app.42458](https://doi.org/10.1002/app.42458)

ARTICLES

Largely toughening biodegradable poly(lactic acid)/thermoplastic polyurethane blends by adding MDI

F. Zhao, H.-X. Huang and S.-D. Zhang, *J. Appl. Polym. Sci.* 2015, DOI: [10.1002/app.42511](https://doi.org/10.1002/app.42511)

Solubility factors as screening tools of biodegradable toughening agents of polylactide

A. Ruellan, A. Guinault, C. Sollogoub, V. Ducruet and S. Domenek, *J. Appl. Polym. Sci.* 2015, DOI: [10.1002/app.42476](https://doi.org/10.1002/app.42476)

Current progress in the production of PLA-ZnO nanocomposites: Beneficial effects of chain extender addition on key properties

M. Murariu, Y. Paint, O. Murariu, J.-M. Raquez, L. Bonnaud and P. Dubois, *J. Appl. Polym. Sci.* 2015, DOI: [10.1002/app.42480](https://doi.org/10.1002/app.42480)

Oriented polyvinyl alcohol films using short cellulose nanofibrils as a reinforcement

J. Peng, T. Ellingham, R. Sabo, C. M. Clemons and L.-S. Turng, *J. Appl. Polym. Sci.* 2015, DOI: [10.1002/app.42283](https://doi.org/10.1002/app.42283)

Biorenewable polymer composites from tall oil-based polyamide and lignin-cellulose fiber

K. Liu, S. A. Madbouly, J. A. Schrader, M. R. Kessler, D. Grewell and W. R. Graves, *J. Appl. Polym. Sci.* 2015, DOI: [10.1002/app.42592](https://doi.org/10.1002/app.42592)

Dual effect of chemical modification and polymer precoating of flax fibers on the properties of the short flax fiber/poly(lactic acid) composites

M. Kodal, Z. D. Topuk and G. Ozkoc, *J. Appl. Polym. Sci.* 2015, DOI: [10.1002/app.42564](https://doi.org/10.1002/app.42564)

Effect of processing techniques on the 3D microstructure of poly(L-lactic acid) scaffolds reinforced with wool keratin from different sources

D. Puglia, R. Ceccolini, E. Fortunati, I. Armentano, F. Morena, S. Martino, A. Aluigi, L. Torre and J. M. Kenny, *J. Appl. Polym. Sci.* 2015, DOI: [10.1002/app.42890](https://doi.org/10.1002/app.42890)

Batch foaming poly(vinyl alcohol)/microfibrillated cellulose composites with CO₂ and water as co-blowing agents

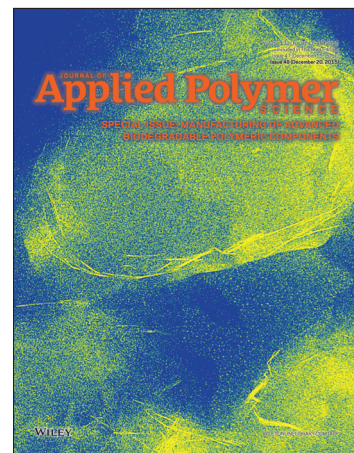
N. Zhao, C. Zhu, L. H. Mark, C. B. Park and Q. Li, *J. Appl. Polym. Sci.* 2015, DOI: [10.1002/app.42551](https://doi.org/10.1002/app.42551)

Foaming behavior of biobased blends based on thermoplastic gelatin and poly(butylene succinate)

M. Oliviero, L. Sorrentino, L. Cafiero, B. Galzerano, A. Sorrentino and S. Iannace, *J. Appl. Polym. Sci.* 2015, DOI: [10.1002/app.42704](https://doi.org/10.1002/app.42704)

Reactive extrusion effects on rheological and mechanical properties of poly(lactic acid)/poly[(butylene succinate)-co-adipate]/epoxy chain extender blends and clay nanocomposites

A. Mirzadeh, H. Ghasemi, F. Mahrous and M. R. Kamal, *J. Appl. Polym. Sci.* 2015, DOI: [10.1002/app.42664](https://doi.org/10.1002/app.42664)



**Special Issue: Manufacturing of Advanced
Biodegradable Polymeric Components**

Guest Editors: Prof. Roberto Pantani (University of Salerno) and
Prof. Lih-Sheng Turng (University of Wisconsin-Madison)

Rotational molding of biodegradable composites obtained with PLA reinforced by the wooden backbone of opuntia ficus indica cladodes

A. Greco and A. Maffezzoli, *J. Appl. Polym. Sci.* 2015, DOI: [10.1002/app.42447](https://doi.org/10.1002/app.42447)

Foam injection molding of poly(lactic) acid: Effect of back pressure on morphology and mechanical properties

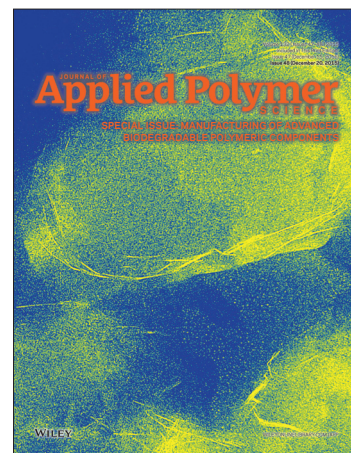
V. Volpe and R. Pantani, *J. Appl. Polym. Sci.* 2015, DOI: [10.1002/app.42612](https://doi.org/10.1002/app.42612)

Modification and extrusion coating of polylactic acid films

H.-Y. Cheng, Y.-J. Yang, S.-C. Li, J.-Y. Hong and G.-W. Jang, *J. Appl. Polym. Sci.* 2015, DOI: [10.1002/app.42472](https://doi.org/10.1002/app.42472)

Processing and properties of biodegradable compounds based on aliphatic polyesters

M. R. Nobile, P. Cerruti, M. Malinconico and R. Pantani, *J. Appl. Polym. Sci.* 2015, DOI: [10.1002/app.42481](https://doi.org/10.1002/app.42481)



Rotational molding of biodegradable composites obtained with PLA reinforced by the wooden backbone of opuntia ficus indica cladodes

Antonio Greco, Alfonso Maffezzoli

Department of Innovation Engineering, University of Salento, 73100 Lecce, Italy

Correspondence to: A. Maffezzoli (E-mail: alfonso.maffezzoli@unisalento.it)

ABSTRACT: This work is aimed to study the suitability of the wooden backbone of opuntia ficus indica cladodes as reinforcement for the production of biodegradable composites by rotational molding. The wooden backbone is extracted from opuntia ficus indica cladodes, which constitute a very relevant agricultural scrap, and is characterized by a thick-walled cellular structure. In view of the potential of poly-lactic acid (PLA) for the production of hollow components by rotational molding, the use of the wooden backbone is expected to increase the stiffness of the material. The wooden backbone of opuntia cladodes can be readily incorporated in the wall thickness of rotational molding products, in contrast to other natural fibers in the form of filaments and/or bundles, which are very difficult to use in the rotational molding. The results obtained showed that, although being characterized by lower properties compared with compression-molded PLA, the bio-composites are characterized by adequate mechanical properties, higher than those previously found for PLA processed by rotational molding. In view of a potential application for the production of fully biodegradable hollow parts, an increase of stiffness and strength can therefore be attained adopting materials and procedure developed in this work. © 2015 Wiley Periodicals, Inc. *J. Appl. Polym. Sci.* **2015**, *132*, 42447.

KEYWORDS: biodegradable; composites; mechanical properties; molding; polyesters

Received 10 February 2015; accepted 30 April 2015

DOI: [10.1002/app.42447](https://doi.org/10.1002/app.42447)

INTRODUCTION

Natural fibers used as reinforcement of composite materials, being characterized by low-cost and low density, are biodegradable and nonabrasive when compared with conventional glass fiber reinforcements. On the other hand, the limited adhesion with hydrophobic polymer matrices, the tendency to form aggregates during processing, and poor resistance to moisture greatly reduce the potential of natural fibers as reinforcement in polymer composites.¹

In recent years natural fibers have attracted the attention of scientists and technologists and a huge number of scientific papers, studying a lot of combination of matrices and natural reinforcements, appeared in the literature. Among other reinforcements, jute,^{2–4} sisal,^{5,6} flax,⁷ bamboo,⁸ banana,⁹ coir,¹⁰ hemp,¹¹ cellulose nanowhiskers,¹² were studied in combination with several thermoplastic and thermosetting matrices. Biodegradable composites, characterized by complete degradation in soil or in composting processes,¹³ are obtained by combination of natural fibers with biodegradable polymers. Among other biodegradable polymers, poly lactic acid (PLA) is the most used, due to its good mechanical properties retained for an adequately long lifetime even in a humid environment.

In view of the production of biodegradable hollow plastic parts, PLA prototypes have been recently built by rotational molding.¹⁴ In order to improve the toughness of PLA, adequately high cooling rates should be attained, therefore reducing the degree of crystallinity of the polymer. In comparison to other polymer processing technologies, rotational molding is severely limited by the difficulty of introducing reinforcing fibers, either continuous^{15,16} or discontinuous.¹⁷ On the other hand, the wooden backbone extracted from the cladodes of opuntia ficus indica acted as an efficient reinforcement in compression molded PLA bio-composites.⁷ The leaves of opuntia ficus indica, called cladodes, constitute a very abundant agricultural scrap, from which different substances can be extracted, for food, dietary and medical applications.¹⁸ Dry cladodes contain a variety of constituents, including minerals (19.6 wt %), waxes and fats (7.2 wt %), lignin (3.6 wt %), and polysaccharides (69.6 wt %), including cellulose (21.6 wt %).¹⁹ The structural function of cladodes is due to the presence of thick walled, lignified xylem and phloem cells, which therefore constitute the wooden backbone of the plant. Such backbone, properly dried and milled, can be a source for the production of wood flour for polymer reinforcement.²⁰ In recent years, the wooden backbone extracted from cladodes, properly treated and dried, has



Figure 1. (a) picture of opuntia ficus indica cladode and (b) of the wooden backbone extracted from cladode. [Color figure can be viewed in the online issue, which is available at wileyonlinelibrary.com.]

found an industrial application for the production of thermal insulating panels.^{21,22}

The aim of this article is to study the possibility of reinforcing rotomolded PLA parts using the wooden backbone of the cladodes of opuntia ficus indica. This porous wood can be readily incorporated in the wall thickness of rotational molding products, in contrast to other natural fibers in the form of filaments and/or bundles, which are very difficult to use in the rotational molding process.

MATERIALS AND METHODS

The wooden backbone was manually extracted from the opuntia ficus indica cladodes after 2 h in boiling water and 3 months drying at room conditions. In Figure 1(a) a picture of a typical opuntia ficus indica cladode is reported. Figure 1(b) shows the lignified xylem and phloem cells (wooden backbone) extracted from the cladode. The SEM image of the opuntia at 27 \times magnification, reported in Figure 2, shows the typical cellular structure of the material. Each cell can be approximated by a rhombic shape, in which the two axes are characterized by an aspect ratio equal to about 2.7 ± 0.7 , obtained as the average of 25 measurements. The structure of the material (whose apparent bulk density is about $330 \pm 30 \text{ kg/m}^3$) resembles that of honeycombs. However, besides the possible use of this wood backbone as core in biodegradable sandwich structures,⁷ its relatively high density and good mechanical properties make the material suitable also as a reinforcement in fully consolidated composites.

The matrix used is a bio-polymer (polylactic acid, PLA), Ingeo Biopolymer 3251D, produced by Nature Works LLC. The grade of PLA was specifically designed for injection molding, and was therefore chosen because of its low viscosity (melt flow rate = 80 g/10 min at 210°C), also suitable for the sintering phenomena governing rotational molding. In order to reduce

the viscosity of PLA, which is considered a key requirement to obtain a good impregnation of the opuntia wooden backbone, 15% by weight of poly ethylene glycol (PEG) plasticizer (molecular weight 400 g/mole) was added to PLA by a twin screw extruder (Haake R Rheomex PTW 16/25 D). The extrusion process was run using the following screw temperature profile: 453-453-453-443-433-417 K and a screw speed of 10 rpm. Materials were pelletized after extrusion. In a previous work, it was shown that addition of 15% PEG plasticizer can reduce the viscosity of PLA, measured at 210°C, from 620 Pa s to 170 Pa s.

In addition, PEG plasticizer usually determines a significant toughening effect on PLA,^{23,24} when the cooling rates are high enough (i.e., in compression molding) to quench the polymer upon cooling. On the other hand, it was shown that, with particular reference to rotational molding, associated with low cooling rates, the plasticizer reduces the toughness. This is due to the increased crystallization kinetics induced by the

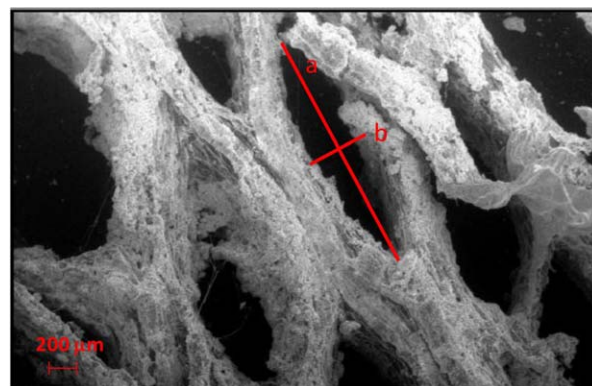


Figure 2. SEM image of the wooden backbone of opuntia ficus indica at $\times 27$ magnification. [Color figure can be viewed in the online issue, which is available at wileyonlinelibrary.com.]

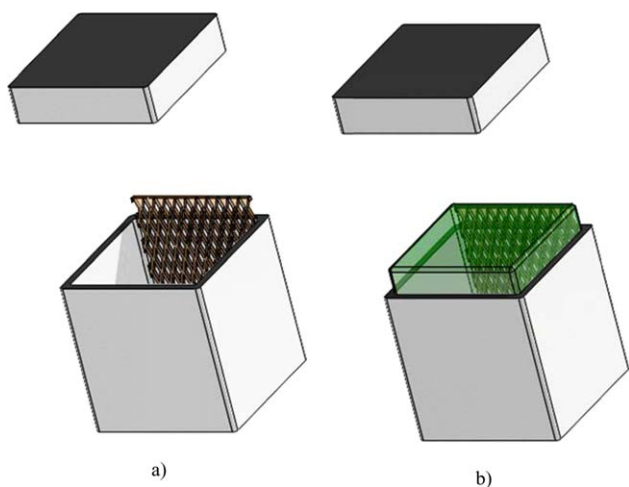


Figure 3. Schematic diagram of the rotational molding process and incorporation of the opuntia in the molten PLA. [Color figure can be viewed in the online issue, which is available at wileyonlinelibrary.com.]

plasticizer. Therefore, a completely amorphous structure can be obtained after processing neat PLA by rotational molding, whereas a semicrystalline structure is obtained with PEG plasticized PLA.¹⁴

Prototypes were built by using a two axis lab scale rotational molding machine designed and produced by Salentec srl (Italy). A squared box-shaped mold was used to fabricate samples characterized by an edge length equal to 148 mm. At the beginning of molding cycle, the opuntia backbone was fixed on the inner mold surface by a silicon glue, as reported in the scheme of Figure 3(a). Then, about 600 g of PLA, corresponding to a theoretical wall thickness of 4 ± 0.15 mm, were placed inside the mold, which was held in rotation for 20 min in a forced convection oven set at 300°C. Measurement of the temperature inside the mold, performed in static conditions, indicated that the temperature attained in the mold after 20 min is about 210°C, which, as previously found,¹⁷ is in the range useful to attain a full polymer sintering. The rotation speed of the primary and the secondary axes were set at 6.1 rpm and 1.6 rpm, respectively. The prototypes were obtained by water cooling and were labeled as RM. During rotational molding of PLA powders, the opuntia backbone is integrated in the wall thickness, as reported in the scheme of Figure 3(b).

A picture of one of the prototypes obtained by rotational molding is reported in Figure 4, showing a very good impregnation of the opuntia backbone, attained during processing. The weight fraction of opuntia, obtained as the ratio between the total mass of opuntia measured before insertion in the mold and the mass of PLA, was estimated to be 2.3%, corresponding to a volume fraction of 4.1%.

For comparison purposes, plasticized PLA sheets reinforced by opuntia backbone were obtained by compression molding, using either a single stage or a double stage process. In single stage process, the material was pressed in a hot press (Campana, Italy) under 20 tons force and 200°C, followed by water cooling of the plates. This procedure required about 35 min for cooling

from 200°C to 40°C, and is therefore characterized by a very slow cooling rate (4°C/min), much lower than that estimated for air cooling of rotational molding (10°C/min¹⁴). The slow cooled samples obtained by this procedure are labeled as CM_SC.

In the double stage process, the material was pre-heated in a forced convection oven up to 200°C, followed by pressing under cold plates at 20 tons force. This procedure required about 5 min for cooling from 200°C to 40°C, and is therefore characterized by a very high average cooling rate (30°C/min), much higher than that estimated for air cooling of rotational molding. The fast cooled samples obtained by this procedure are labeled as CM_FC.

X-ray analysis was performed on opuntia wooden backbone and PLA bio-composites, within the range $2\theta = 5^\circ - 35^\circ$, using a Wide angle X-ray Diffractometer, RIGAKU Ultima +.

Differential scanning calorimetry (DSC) analysis was performed on a Mettler Toledo 822 instrument under a nitrogen flux of 30 mL min⁻¹ applying a heating scan between 20°C and 210°C at 20°C/min. In order to account for the different cooling rates which can be attained at different distances from the mold wall, samples extracted from the rotomolded prototypes were cut on the whole thickness. In fact, the mold side of the prototype is expected to experience higher cooling rates, which could result in lower degree of crystallinity, compared to the air side.²⁵ Sample extraction across the whole prototype thickness is necessary in order to obtain the average value of the degree of crystallinity attained at the end of cooling during rotational molding experiments.

In plane tensile tests were performed on opuntia wooden backbones using a Lloyd LR 5K instrument according to ASTM C297-94 standards, with a cross head speed of 0.5 mm/min, on rectangular (15 mm × 95 mm) samples. Before testing, the grip zones of the sample were impregnated with PP in order to prevent slipping and rupture.

In plane compression tests were performed on opuntia, in directions parallel and perpendicular to grain. In both cases, an



Figure 4. Picture of sample extracted from a rotational molded prototype. [Color figure can be viewed in the online issue, which is available at wileyonlinelibrary.com.]

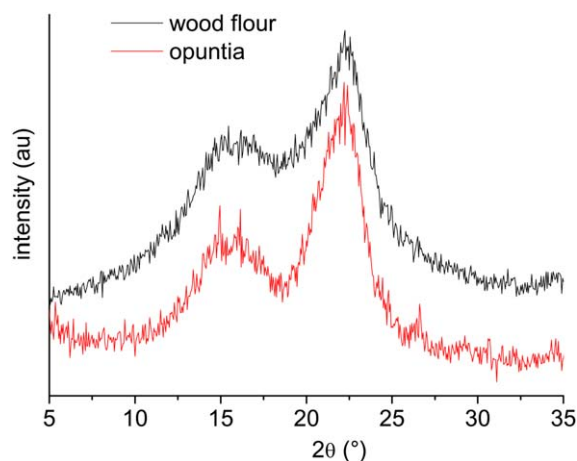


Figure 5. X-ray diffraction patterns of wood flour and opuntia ficus indica wooden backbone. [Color figure can be viewed in the online issue, which is available at wileyonlinelibrary.com.]

unsupported gage section, according to ASTM D3410-95, was used, on 15 mm × 95 mm rectangular samples.

Flexural tests were performed on opuntia wooden backbone, and on compression-molded and rotational-molded prototypes, according to ASTM D790-00, using a crosshead speed of 1 mm/min and a span to thickness ratio equal to 16.

A Scanning Electron Microscope Zeiss EVO 40 SEM instrument was used for the morphological characterization of opuntia wooden backbone.

RESULTS AND DISCUSSION

The XRD patterns of opuntia wooden backbone are reported in Figure 5, and compared with those of wood flour. The two patterns are essentially the same, and are made of a halo band, due to the presence of amorphous lignin and polysaccharides, and a crystalline peak at $2\theta = 22.2^\circ$, due to crystalline cellulose.

X-ray diffraction patterns of samples CM_SC and CM_FC, reported in Figure 6, show the presence of a PLA crystalline

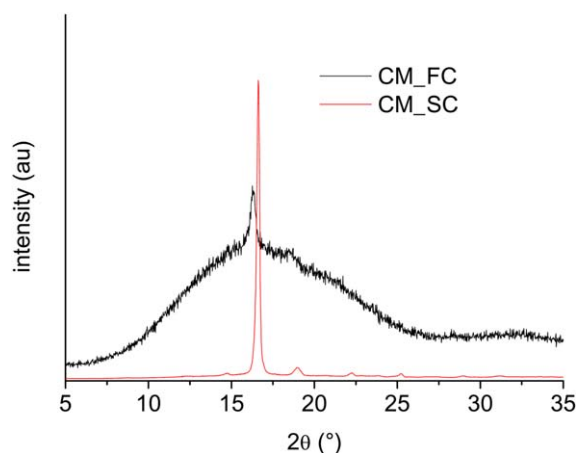


Figure 6. X-ray diffraction patterns of compression-molded PLA composites. [Color figure can be viewed in the online issue, which is available at wileyonlinelibrary.com.]

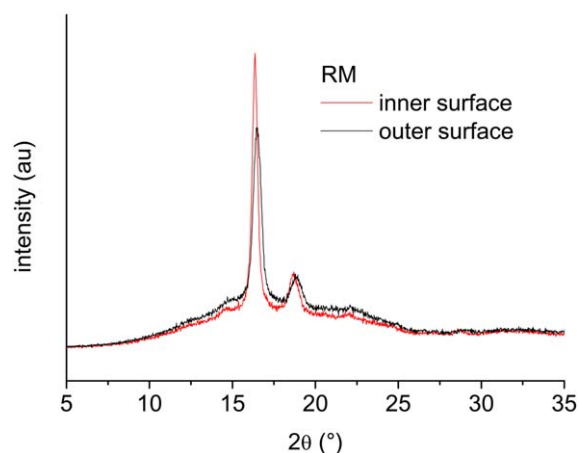


Figure 7. X-ray diffraction patterns of rotational-molded PLA composites. [Color figure can be viewed in the online issue, which is available at wileyonlinelibrary.com.]

phase, as evidenced by the peaks at $2\theta = 16.5^\circ$ and $2\theta = 18.7^\circ$, which are assigned to the crystal planes (200)/(110) and (203) of the α form, respectively.²⁶ Referring to the peak at 16.5° , the intensity for sample CM_SC is much higher than that observed for sample CM_FC. The fraction of crystalline phase was evaluated as the ratio between the area of the peaks at 16.5° and 18.7° , and the total area of the XRD pattern, including the amorphous halo band. A value of the degree of crystallinity equal to 0.028 ± 0.003 and 0.51 ± 0.061 was calculated for CM_FC and CM_SC, respectively. Further, the unperturbed crystallite length in the normal direction of the (200/110) reflection plane was calculated from the full width at half maximum (FWHM) of the crystalline peak, using the Debye Scherrer equation.²⁶ A value of 0.32 ± 0.028 nm and 0.65 ± 0.10 nm were found for CM_FC and CM_SC, respectively. The higher degree of crystallinity and the larger crystals of CM_SC are due to the much lower cooling rate during processing compared to CM_FC.

The XRD, reported in Figure 7, are obtained on PLA extracted from the outer surface (in direct contact with the mold during the process) and from the inner surface (in contact with air) of the sample processed by rotational molding. The sample extracted from the outer surface shows a less intense crystalline peak compared to the sample extracted from the inner surface, as a consequence of the lower degree of crystallinity, resultant from the higher cooling rate experienced by the surface in contact with the mold. The degree of crystallinity is estimated to be 0.28 ± 0.01 and 0.22 ± 0.01 for the samples extracted from the inner surface and the outer surface, respectively. In any case, the degree of crystallinity of rotational-molded PLA is higher than the degree of crystallinity of PLA processed by double stage compression molding, and lower than that of PLA processed by single stage compression molding.

The DSC analysis performed on compression molded and rotational molded PLA prototypes are reported in Figure 8. The most relevant thermal properties, i.e., glass transition temperature T_G , cold crystallization enthalpy and peak temperature, ΔH_{CC} and T_{CC} , melting enthalpy and peak temperature, ΔH_M

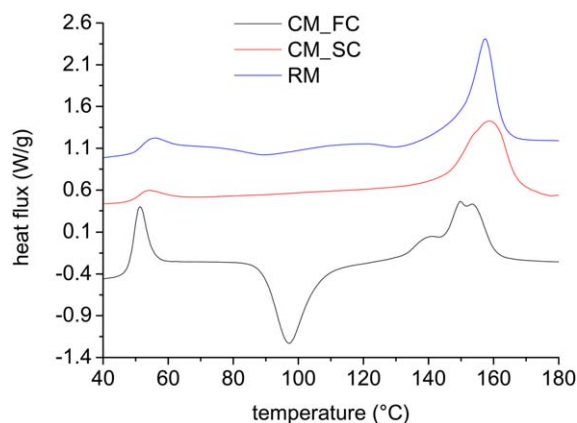


Figure 8. DSC traces of PLA composites. [Color figure can be viewed in the online issue, which is available at wileyonlinelibrary.com.]

and T_M , are reported in Table I. The glass transition signal of CM_FC sample observed at about 47°C, includes an endothermic peak, which evidences that structural relaxation phenomena occurred below glass transition.^{27,28} At higher temperatures, a cold crystallization peak, a direct consequence of the very low degree of crystallinity attained during compression molding, is characterized by an area ΔH_{CC} . Finally, at about 155°C, the endothermic peak, due to melting of the polymer, is characterized by a heat of fusion ΔH_M . Since the melting process involves both the melt crystallized and the cold crystallized fractions, it is possible to write that:

$$\Delta H_M = \Delta H_{MC} + \Delta H_{CC} \quad (1)$$

Where ΔH_{MC} is the melt crystallization enthalpy (attained during cooling of the material). The initial degree of crystallinity of each sample, resulting from the cooling conditions during processing, can be therefore obtained as:

$$x_C = \frac{\Delta H_M - \Delta H_{CC}}{\Delta H^0} \quad (2)$$

where ΔH^0 is the melting enthalpy of a completely crystalline PLA, equal to 93 J/g.²⁹ The thermogram of Figure 8 and the data of Table I show that for sample CM_FC, $\Delta H_M \cong \Delta H_{CC}$, indicating that the initial degree of crystallinity is negligible, in very good agreement with XRD analysis results, which allowed to estimate a degree of crystallinity of 2%.

The DSC thermogram of sample CM_SC, also reported in Figure 8, differs from that of sample CM_FC mainly for the absence of the cold crystallization peak, and, as evident from Table I, for the very high value of the melting enthalpy. The absence of cold crystallization, according to eq. (1), indicates that melting only concerns the melt crystallized fraction origi-

Table I. Thermal Properties of PLA Matrix Composites

	T_G (°C)	T_{CC} (°C)	ΔH_{CC} (J/g)	T_M (°C)	ΔH_M (J/g)
CM_FC	47.1	97.4	35.5	149.0	35.3
CM_SC	47.8	//	//	158.0	47.1
RM	52.1	89.4	7.2	156.3	35.8

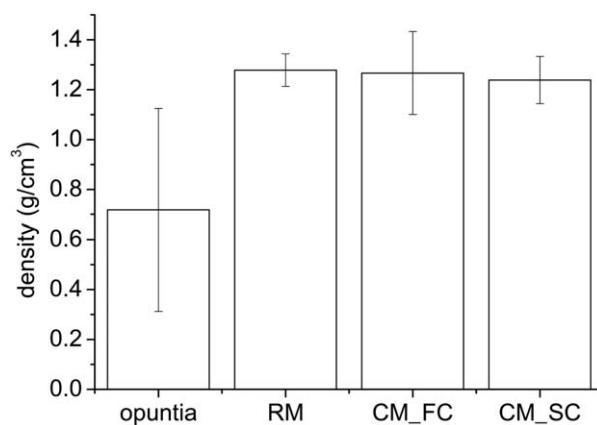


Figure 9. Density of PLA composites.

nated from cooling during compression molding. The data of Table I can be used to estimate by eq. (2) an initial value of the degree of crystallinity equal to 0.50, which is again a value in excellently good agreement with the value found from XRD analysis, i.e., 0.51. The very slow cooling rate experienced by CM_SC sample, is also responsible for the formation of very thick crystalline lamellae, as evidenced by the very high value of the melting temperature. Finally, the DSC thermogram of sample RM shows an intermediate behavior between that of CM_SC and CM_FC. In fact, cold crystallization occurs, but its enthalpy is lower than that of sample CM_FC. Application of eq. (2) with the data of Table I leads to an initial degree of crystallinity equal to 0.30, which is in fairly good agreement with the results from XRD analysis. The relatively high value of melting temperature indicates, also for this sample, the presence of thick lamellae, resulting from relatively low cooling rate.

The density of the three samples is reported in Figure 9 together with that of the opuntia wooden backbone. This last is characterized by a relatively low density, compared to lignin and cellulose, indicating the existence of a very porous structure within cell walls. On the other hand, the PLA biocomposites are characterized by comparable densities, around 1.23–1.26 g/cm³, (which is in the range of density reported in the material technical data sheet). Using the rule of mixtures, with a measured volume fraction of opuntia equal to 0.04, a density of PLA and opuntia equal to 1.24 and 0.7 g/cm³ respectively, the theoretical density of the biocomposite processed by rotational molding, was estimated to be 1.22 g/cm³, which is a value very close to the density of neat PLA. Therefore, addition of opuntia, in very low amounts, does not contribute to significantly modify the density of the biocomposite. In view of the mechanical characterization, the most relevant result is that the PLA composite processed by rotational molding is characterized by the same density as the compression molded PLA. This is confirmed by ANOVA³⁰ performed on the density measurements. With 3 factor levels (different processing, i.e. rotational molding, double stage and single stage compression molding) and 29 degrees of freedom for each level (30 tests on each level) it is possible to estimate a critical value of the F ratio ($F_{cv}=2.87$) equal to 3.1 at a significance level $\alpha=0.05$. The F ratio value of density measurement is 0.52, which is much lower than F_{cv} (2.27),

Table II. Mechanical Properties of Wooden Backbone of *Opuntia Ficus Indica*

	Elastic modulus (MPa)	Strength (MPa)	Deformation at break (%)
Tensile parallel	157 ± 55	6.3 ± 2.3	1.4 ± 0.51
Compression parallel	610 ± 72	21.5 ± 5.8	No break
Compression transversal	15 ± 2	0.42 ± 0.2	No break
Flexural	354 ± 168	4.65 ± 0.9	0.031 ± 0.0219

indicating that differences are not relevant at the 5% significance level. In agreement with the observation of Figure 4, the high value of density of rotational molded biocomposites indicates the absence of voids, which is in turn due to the good combination of material viscosity and processing conditions, allowing for an efficient impregnation of the wooden backbone by the molten polymer.

In-plane properties of opuntia were assessed by tensile and compressive measurements. Tensile properties, measured in the longitudinal direction (parallel to the a axis reported in Figure 2) are reported in Table II. Compression properties, measured in the longitudinal and transversal direction (parallel to the a and b axis of Figure 2, respectively), are also reported in Table II. Compression properties in the longitudinal direction are much higher than those measured in the transversal direction. The flexural properties of opuntia reflect both the tensile and the compressive behavior of the material. In fact, the flexural modulus is between tensile and compressive modulus. In any case, the mechanical properties are characterized by a very high standard deviation, which is essentially related to the heterogeneous structure of the material, as clearly evident in Figure 1.

In order to highlight the potential increase of mechanical properties due to the presence of the opuntia, the stiffness of the backbone E^{eff} can be related to the stiffness of the wooden structural elements in the cladodes, E_s . Accounting for the rhombic geometry shown in Figure 2 the following relationship is obtained:³¹

$$\frac{E^{\text{eff}}}{E_s} = \frac{4}{\sqrt{3} \left[1 + \left(\frac{t}{L}\right)^2 (2(1+\nu_s) + 3) \right]} \left(\frac{t}{L}\right)^3 \quad (3)$$

where t is the thickness of the cell wall, L is the characteristic length of the cell and ν_s the Poisson ratio of the constituent material, taken equal to 0.35. From the optical microscopy analysis, $t/L = 0.3$, and with a flexural modulus of 350 MPa (obtained as the average between tensile and compressive modulus) the modulus of the constituent material of the backbone can be estimated to be $E_s = 8.6$ GPa, and is therefore much higher than the modulus of the biopolymer, indicating the potential reinforcing efficiency of the material.

The stress–strain curves obtained from flexural tests on PLA biocomposites are reported in Figure 10 and the calculated properties in Table III. All samples exhibit a brittle behavior, in contrast to what is usually observed for compression-molded plasticized PLA. The brittleness of the rotational molded prototypes can be explained by considering that, under the processing conditions typical of rotational molding, the plasticized PLA is

highly crystalline.¹⁴ On the other hand, the brittleness of compression molded composite prototypes is attributed to the presence of the reinforcement.⁷

A comparison between CM_FC and CM_SC shows that the latter is characterized by a higher modulus and lower strength and elongation at break. Both effects can be explained with the increase of the degree of crystallinity and of crystal size, as formerly observed by XRD and DSC analysis.

Rotational molded PLA bio-composite is characterized by lower modulus in comparison to compression molded PLA. The strength of RM is comparable to that of CM_SC, and the elongation at break of RM is comparable to that of CM_FC. However, comparison between the bio-composite and plasticized PLA, reported in a previous work,¹⁴ indicate that the introduction of opuntia wooden backbone involves an increase of the flexural modulus of plasticized PLA from 1.4 GPa to 1.7 GPa, and an increase of the flexural strength from 20 MPa to 32 MPa. On the other hand, the deformation at break is decreased from 2.9% to 2.1%. Also, the toughness is increased from 0.40 to 0.44 mJ/mm³.

Applying simple micromechanics rule of mixture for the calculation of the modulus of the composite, E_c , assuming unidirectional reinforcement (Figures 1 and 2) is equal to $E_c = 1.7$ GPa with $E_m = 1.4$ GPa, $E_s = 8.6$ GPa, and $\nu_f = 0.04$. This value is the same as the experimental value, indicating that the maximum reinforcing efficiency is attained by the developed procedure with $\nu_f = 0.04$.

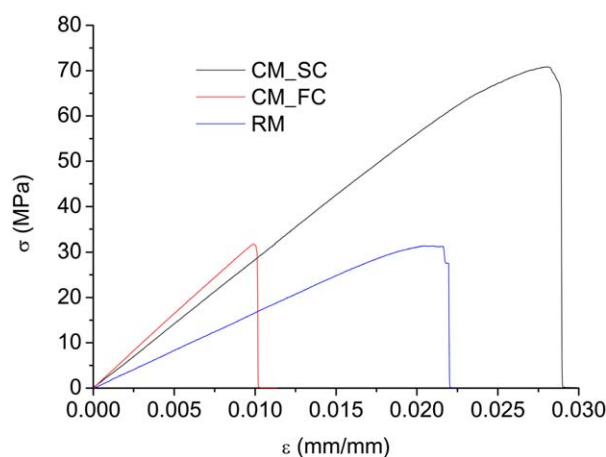


Figure 10. Stress–strain curves of PLA bio-composites. [Color figure can be viewed in the online issue, which is available at wileyonlinelibrary.com.]

Table III. Mechanical Properties of PLA Bio-Composite

	Flexural modulus (GPa)	Flexural strength (MPa)	Deformation at break (%)
CM_FC	2.9 ± 0.85	67 ± 11.4	2.6 ± 0.2
CM_SC	3.1 ± 0.20	30 ± 7.0	1.0 ± 0.1
RM	1.7 ± 0.5	32 ± 10.6	2.1 ± 0.3

This result highlights the very good adhesion between reinforcing backbone and PLA. In fact, in a previous work, the interlaminar shear strength in a sandwich structure made with opuntia wooden backbone core and PLA skin was found to be about 14 MPa, which is a very high value, much higher than the adhesion strength of glass³² or carbon³³ fibers to epoxy resins, and comparable to the adhesion strength of UHMWPE fibers to LDPE matrix.³⁴

It should be emphasized, however, that, depending on the density of the wooden backbone, and therefore on the cell wall thickness and their characteristic length, a maximum volume fraction of opuntia exists. Considering that the fractional volume of voids in the wooden backbone is given as:³¹

$$x_v = 1 - \frac{2}{\sqrt{3}} \frac{t}{L} \quad (4)$$

It follows that for the wooden backbone used in this work, the minimum amount of matrix required in order to completely fill the voids, being $t/L = 0.3$, is $v_m = 0.66$. Since micromechanics can be successfully applied to the calculation of elastic modulus of opuntia wood reinforced composites, the maximum modulus of the composite which can be attained is 3.9 GPa.

CONCLUSIONS

In this work, the wooden backbone of opuntia ficus indica cladodes is used as reinforcement for bio-composites processed by rotational molding. Rotational molding allows the use of the wooden backbone for the production of complex shapes, while compression molding, which allows to produce plane sheets or shapes characterized by low curvatures. The PLA matrix was modified by the addition of a plasticizer, in order to reduce the viscosity of the material, thus allowing an efficient impregnation of the wooden fibers during rotational molding.

A void free composite is obtained, by a proper combination of material viscosity and processing parameters. The PLA matrix processed by this method is characterized by a semicrystalline structure, as evidenced by XRD and DSC analysis, even if high cooling rates are attained by the use of water as cooling system.

The biocomposite produced by rotational molding is characterized by mechanical properties comparable to those of PLA processed by compression molding, which is characterized by cooling rates comparable to those found in rotational molding with water cooling (20–30°C/min).

A comparison with plasticized PLA processed by rotational molding, which has been studied in a previous work, shows that reinforcement with the opuntia backbone leads to an increase of stiffness, strength and toughness.

REFERENCES

- Nabi Saheb, D.; Jog, J. P. *Adv. Polym. Technol.* **1999**, *18*, 351.
- Gowda, T. M.; Naidu, A. C. B.; Chhaya, R. *Compos. Part A* **1999**, *30*, 277.
- Maffezzoli, A.; Calò, E.; Zurlo, S.; Mele, G.; Tarzia, A.; Stifani, C. *Compos. Sci. Technol.* **2004**, *64*, 839.
- Campaner, P.; D'Amico, D.; Ferri, P.; Longo, L.; Maffezzoli, A.; Stifani, C.; Tarzia, A. *Macromol. Symp.* **2010**, *296*, 526.
- Li, Y.; Mai, Y. W.; Ye, L. *Compos. Sci. Technol.* **2000**, *60*, 2037.
- Nunez, A. J.; Aranguren, M. I.; Berglund, L. A. *J. Appl. Polym. Sci.* **2006**, *101*, 1982.
- Greco, A.; Gennaro, R.; Timo, A.; Bonfantini, F.; Maffezzoli, A. *J. Polym. Environ.* **2013**, *21*, 910.
- Okubo, K.; Fujii, T.; Yamamoto, Y. *Compos. Part A* **2004**, *35*, 377.
- Joseph, S.; Sreekala, M. S.; Oommen, Z.; Koshyc, P.; Thomas, S. *Compos. Sci. Technol.* **2002**, *62*, 1857.
- Esmeraldo, M. A.; Barreto, A. C.; Freitas, J. E. B.; Fachine, P. B. A.; Sombra, A. S. B.; Corradini, E.; Mele, G.; Maffezzoli, A.; Mazzetto, S. E. *BioResources* **2010**, *5*, 2478.
- Mehta, G.; Drzal, L. T.; Mohanty, A. K.; Misra, M. *J. Appl. Polym. Sci.* **2010**, *99*, 1055.
- Fortunati, E.; Peltzer, M.; Armentano, I.; Torre, L.; Jiménez, A.; Kenny, J. M. *Carbohydr. Polym.* **2012**, *90*, 948.
- Lee, S. H.; Wang, S. *Compos. Part A* **2006**, *37*, 80.
- Greco, A.; Maffezzoli, A. *Adv. Polym. Technol.* **2015**, doi: 10.1002/adv.21505
- Salomi, A.; Greco, A.; Felling, F.; Manni, O.; Maffezzoli, A. *Adv. Polym. Technol.* **2007**, *26*, 21.
- Greco, A.; Romano, G.; Maffezzoli, A. *Compos. Part B-Eng* **2014**, *56*, 157.
- Greco, A.; Maffezzoli, A.; Forleo, S. *Thermochim Acta* **2014**, *582*, 59.
- Saenz, C. *J. Arid Environ.* **2000**, *46*, 209.
- Malainine, M. E.; Dufresne, A.; Dupeyre, D.; Mahrouza, M.; Vuonga, R.; Vignon, M. R. *Carbohydr. Polym.* **2003**, *51*, 77.
- Malainine, M. E.; Mahrouz, M.; Dufresne, A. *Macromol. Mater. Eng.* **2004**, *289*, 855.
- Colajanni, S.; De Vecchi, A.; Fiore, V.; Lanza Volpe, A.; Valenza, A. Materiale isolante a base di cactacee, pannello realizzato con detto materiale e relativo processo di produzione, Italian patent IT2010RM00355 20100630.

22. Albamonte, F. Realizzazione di pannelli isolanti termico-acustici per l'edilizia a base di legno di opunzia, Italian Patent IT2008PA00023 20081016.
23. Kulinski, Z.; Piorkowska, E. *Polymer* **2005**, *46*, 10290.
24. Hu, Y.; Hu, Y. S.; Topolkaev, V.; Hiltner, A.; Baer, E. *Polymer* **2003**, *44*, 5681.
25. Crawford, R. J. *J. Mater. Process Tech.* **1996**, *56*, 263.
26. Zhang, X.; Schneider, K.; Liu, G.; Chen, J.; Brüning, K.; Wang, D.; Stamm, M. *Polymer* **2011**, *52*, 4141.
27. Greco, A.; Gennaro, R.; Rizzo, M. *Polym. Int.* **2012**, *61*, 1326.
28. Greco, A.; Rizzo, M.; Maffezzoli, A. *Thermochim. Acta* **2012**, *543*, 226.
29. Battagazzore, D.; Bocchini, S.; Frache, A. *Express Polym. Lett.* **2011**, *5*, 849.
30. Montgomery, D. C. *Introduction to Statistical Quality Control*, 2nd ed.; Wiley: New York, **1991**.
31. Chen, D. H.; Ozaki, S. *Compos. Struct.* **2009**, *88*, 17.
32. Etcheverry, M.; Ferreira, M. L.; Capiati, N. J.; Pegoretti, A.; Barbosa, S. E. *Compos. Part A-Appl. S* **2008**, *39*, 1915.
33. Greco, A.; Maffezzoli, A.; Buccoliero, G.; Caretto, F.; Cornacchia, G. *J. Compos. Mater.* **2013**, *47*, 369.
34. Devaux, E.; Cazé, C. *Compos. Sci. Technol.* **1999**, *59*, 879.